

Conductance Peak Distributions in Quantum Dots at Finite Temperature: Signatures of the Charging Energy

Y. Alhassid, M. Gökçedağ and A.D. Stone

*Center for Theoretical Physics, Sloane Physics Laboratory, Yale University, New Haven,
Connecticut 06520, USA*

(submitted July 17, 1997)

Abstract

We derive the finite temperature conductance peak distributions and peak-to-peak correlations for quantum dots in the Coulomb blockade regime assuming the validity of random matrix theory. The distributions are universal, depending only on the symmetry class and the temperature measured in units of the mean level spacing, Δ . When the temperature is comparable to Δ several resonances contribute to the same conductance peak and we find significant deviations from the previously known $T \ll \Delta$ distributions. In contrast to the $T \ll \Delta$ case, these distributions show a strong signature of the charging energy and charge quantization on the dot.

PACS numbers: 73.40.Gk, 05.45+b, 73.20.Dx, 24.60.-k

Quantum dots are two-dimensional microstructures of micron scale or smaller in which a small number of electrons are confined by electrostatic potentials. They can be fabricated with relatively little intrinsic disorder, in which case the motion of the electrons is ballistic. The transport properties of such dots are measured by coupling them to leads through point contacts. As the contacts are pinched off, the dot becomes more closed (i.e. more weakly coupled to the leads) and the electron resonances become well-isolated. For temperatures that are low compared with the mean level spacing, the dot's conductance is dominated by the resonance that is closest to the Fermi energy of the electrons in the leads. Since a tunneling event requires the addition of one electron into the dot and a collective charging energy of e^2/C (where C is the capacitance of the dot), the conductance exhibits a series of approximately equally spaced peaks as a function of the gate voltage [1]. The height of the conductance peaks, however, shows order of magnitude fluctuations. These fluctuations measure directly the fluctuations of the wavefunctions in the interface region between the dot and the leads. Using random matrix theory (RMT), the statistical distribution of conductance peak heights was derived in closed form [2]. Recently, these distributions were measured in dots with single-channel symmetric leads and several hundred electrons, for both the case of conserved and broken time-reversal symmetry [3,4], and were found to be in good agreement with the theoretical predictions. The measured parametric correlator of the conductance peak as a function of an applied magnetic field was also found to be in agreement with the predicted correlator [5].

One aspect of the data from ref. [4] has remained unexplained. Strong correlations were observed between the heights of adjacent peaks, in contrast to the RMT prediction of vanishing correlations in the low temperature limit. In this experiment the temperature was estimated to be $0.3 - 0.5\Delta$, so the correlations could be due to deviations from the $T \ll \Delta$ results; but then the rather good agreement of the conductance distributions with the $T \ll \Delta$ result is somewhat puzzling. We address these questions here by deriving conductance peak distributions and peak-to-peak correlations for temperatures that are not much smaller than the mean-level spacing Δ . We find that, due to effects of the charging energy, the corrections

to the distributions are smaller than expected from the non-interacting Landauer-Büttiker conductance formula [6]. Nonetheless significant peak-to-peak correlations are induced, and we will discuss their relation to experiment below. The deviation of the finite temperature distributions from those predicted by naive application of the Landauer-Büttiker formula is somewhat surprising since on resonance the mean interaction energy difference between the N and $N - 1$ particle ground states vanishes [7,8] and indeed in the limit $T \ll \Delta$ one obtains exactly the same distribution as in the non-interacting case [9,10]. Our result is derived by combining the theory of sequential resonant tunneling in the Coulomb blockade regime [7,8] with the statistical assumptions of RMT.

Beenakker [7] considered the linear response of a dot in equilibrium with a chemical potential equal to the Fermi energy in the leads. The electrostatic energy of the dot with N electrons is given by $U(N) = (Ne)^2/2C - Ne\alpha V_g$ where C is the capacitance of the dot, V_g is the gate voltage and α denotes the ratio between the plunger gate to dot capacitance and the total capacitance. The Fermi energy of a resonant tunneling event of the N -th electron into the dot is given by the condition $E_F = U(N) - U(N - 1) + E_N$, where E_N is the single-particle energy of the N -th level. Alternatively we can define an effective Fermi energy $\tilde{E}_F = E_F + e\alpha V_g$ for which the condition of resonant tunneling is $\tilde{E}_F = E_N + (N - 1/2) e^2/C$. If the gate voltage is tuned to satisfy $e\alpha V_g = (N - 1/2) e^2/C$ one reaches the degeneracy condition for which the charging energy $U(N) - U(N - 1)$ vanishes (to order Δ). Assuming this condition, and that T is always greater than the resonance width, Beenakker showed that the resonant conductance $G(T, \tilde{E}_F)$ can be written as a weighted sum over the $T = 0$ resonances λ in the dot

$$G(T, \tilde{E}_F) = \frac{e^2}{h} \frac{\pi \bar{\Gamma}}{4kT} g \quad \text{where } g = \sum_{\lambda} w_{\lambda}(T, \tilde{E}_F) g_{\lambda} . \quad (1)$$

Here $g_{\lambda} = 2\bar{\Gamma}^{-1}[\Gamma_{\lambda}^l \Gamma_{\lambda}^r / (\Gamma_{\lambda}^l + \Gamma_{\lambda}^r)]$ are the level conductances, where $\Gamma_{\lambda}^{l(r)}$ is the width of a resonance level λ to decay into the left (right) lead and $\bar{\Gamma} = \bar{\Gamma}^l + \bar{\Gamma}^r$ is the total average width. The quantity g_{λ} is dimensionless and temperature-independent. $w_{\lambda} = w_{\lambda}(T, \tilde{E}_F)$ is the weight with which a given resonance λ contributes to the conductance. The contribution

to w_λ from any fixed number of electrons on the dot is the product of the probability that the level E_λ is filled with the dot having that number of electrons, and the probability that there is an empty state in the leads at the corresponding total energy [7]:

$$w_\lambda = \sum_N 4P_N \langle n_\lambda \rangle_N \left[1 - f \left(E_\lambda + (N - 1/2) \frac{e^2}{C} - \tilde{E}_F \right) \right]. \quad (2)$$

P_N is the probability that the dot has N electrons, $\langle n_\lambda \rangle_N$ is the *canonical* occupation of a level λ , and $f(\epsilon) = [1 + \exp(\epsilon/kT)]^{-1}$. In many experiments $T, \Delta \ll e^2/C$ and only one term in (2) contributes to a given conductance peak, corresponding to N_0 electrons in the dot. Eq. (2) reduces to [7]

$$w_\lambda = 4f(\Delta F_{N_0} - \tilde{E}_F) \langle n_\lambda \rangle_{N_0} \left[1 - f(E_\lambda - \tilde{E}_F) \right], \quad (3)$$

where $\Delta F_N = F_N - F_{N-1}$ and F_N is the canonical free energy of N non-interacting particles. Here and in the following $e\alpha V_g$ is measured relative to $(N_0 - 1/2)e^2/C$.

In the limit $T \ll \Delta$ only the central level $\lambda = N_0$ (denoted by $\lambda = 0$ in the following) contributes to a given conductance peak in (1). Its weight w_0 becomes the appropriate weight for non-interacting electrons, which one would get by appropriate approximation of the Landauer-Büttiker formula for narrow isolated resonances

$$w_0^{LB} = 4kT f'(E_0 - \tilde{E}_F) = \cosh^{-2} \left(\frac{E_0 - \tilde{E}_F}{2kT} \right). \quad (4)$$

In the absence of interactions this result generalizes trivially to the regime where T is not much smaller than Δ . In this case several resonances λ contribute to (1) with weights w_λ^{LB} obtained by replacing E_0 in (4) with E_λ . Since the charging energy “vanishes” on resonance one might have expected Eq. (2) to reduce to this form. In fact this only happens when $e^2/C \ll \Delta$; not in the experimentally relevant limit $e^2/C \gg \Delta$. If $e^2/C \rightarrow 0$, then all terms (with various number of electrons N) contribute to (2). The factor $1 - f$ becomes independent of N and by definition $\sum_N P_N \langle n_\lambda \rangle_N = f(E_\lambda - \tilde{E}_F)$ is just the grand-canonical occupation number, so that w_λ reduces to w_λ^{LB} for all λ 's. In this case the various manifolds of many-electron levels with $N_0, N_0 \pm 1, N_0 \pm 2; \dots$ electrons on the dot differ from each

other only by an energy of order Δ , and consequently many of the P_N are non-negligible and contribute to w_λ . However, when the charging energy is large compared with Δ only two manifolds (N_0 and $N_0 - 1$) are degenerate while all others are pushed away amounts of order e^2/C . Consequently, the weights w_λ differ significantly from their non-interacting values when $T \sim \Delta$.

We now evaluate these differences quantitatively. This requires the calculation of the canonical quantities F_N and $\langle n_\lambda \rangle_N$ in (3), through a projection on a fixed number of particles N . This is done in terms of an exact quadrature formula [11] that expresses the canonical partition function $Z_N = e^{-F_N/T}$ in terms of grand-canonical partition functions

$$Z_N = \frac{e^{-\beta E_g}}{N_{sp}} \sum_{m=1}^{N_{sp}} \prod_{i=1}^{N_{sp}} \left(1 + e^{-\beta |E_i - \mu|} e^{i\sigma_i \phi_m} \right). \quad (5)$$

Here the quadrature points are $\phi_m = 2\pi m/N_{sp}$ (N_{sp} is the number of single-particle states), and μ is a chemical potential chosen anywhere in the range $E_N \leq \mu < E_{N+1}$. $E_i - \mu$ are just the particle ($i > \mu$) or hole ($i \leq \mu$) energies, and $\sigma_i = 1$ for a hole and -1 for a particle. Since the factors in each term in (5) decay exponentially as we move away from μ , only a finite number of single-particle states N_{sp} around μ are needed for an exact calculation. The canonical occupations are calculated by a similar projection method and differ significantly from the corresponding Fermi-Dirac occupations at temperatures of order Δ or less. They lie on a curve similar in shape to the a Fermi-Dirac distribution with a chemical potential of $\mu = (E_N + E_{N+1})/2$, but with a level-dependent effective temperature which in the vicinity of μ is smaller than the actual temperature by almost a factor of 2 [12]. The inset to Fig. 1 shows both distributions for $T = 0.5\Delta$ assuming a uniformly spaced (picket-fence) spectrum.

While the numerical calculations below include fluctuations of the single-particle energies, their effect turns out to be quite small, so that the simple picket-fence spectrum can be used to illustrate and understand the results. For a picket-fence spectrum $\Delta F_N = E_N$ and $P_N = f(E_N - \tilde{E}_F)$. In Fig. 1 we show the weights $w_\lambda(T, \tilde{E}_F)$ versus \tilde{E}_F for $T = 0.5\Delta$ for several levels around the central level $\lambda = 0$. The functions w_λ become shallower and broader as we move away from the level $\lambda = 0$, in contrast to the shape of the Landauer-Büttiker

weights (4), which is independent of λ . Assuming the conductance peaks at $\tilde{E}_F = E_0$ we also show in Fig. 1 the weights $w_\lambda \equiv w_\lambda(T, E_0)$ that contribute to the conductance peak height vs. E_λ [13].

For the picket-fence spectrum $P_{N_0} = 1/2$ and $w_0 = \langle n_0 \rangle_{N_0}$ (denoted in the following by $\langle n_0 \rangle$); whereas for all levels $\lambda \neq 0$, the relation $w_\lambda \approx w_\lambda^{LB}/2$ holds to within 20% or better. Since $\langle n_0 \rangle < 1 = w_0^{LB}$ the actual weights (and hence the conductance) are always smaller than predicted by the non-interacting theory. Hence in a rather subtle manner the charging energy manifests itself in a suppression of the finite temperature conductance and its fluctuations. In the limit $T \gg \Delta$ the weight for the central level $w_0 = \langle n_0 \rangle \rightarrow 1/2 = w_0^{LB}/2$ (see left inset of Fig. 1), and we recover the classical result [7] $G \approx G^{LB}/2$. In fact we find that this limit is practically reached at $T \approx 2\Delta$ where w_0 is within 20% of 1/2. However a second interesting effect occurs for $0.1\Delta < T < 2\Delta$. In this interval $\langle n_0 \rangle > 1/2$ and the ratio w_λ/w_λ^{LB} is enhanced for the central level relative to adjacent levels. Thus effectively the distribution of g is less sensitive to temperature than would be expected from the non-interacting theory.

To test this notion quantitatively we calculated the conductance distributions from Eqs. (1)–(2) and compared them to the non-interacting distributions. A statistical theory of the conductance in irregularly shaped quantum dots was developed in Ref. [2] in the limit $T \ll \Delta$. The partial width amplitude to decay into a channel c from a resonance level λ is expressed as the projection of the resonance wavefunction on the channel wavefunction across the interface between the dot and the lead. When the electron dynamics in the dot is chaotic, the statistical fluctuation of the resonance wavefunction are well described by RMT, and the universal distributions of the dimensionless level conductance g_λ can be derived. For $T \ll \Delta$ and single-channel leads, $P(g) = \sqrt{2/\pi} g e^{-2g}$ for conserved time-reversal symmetry (GOE) and $P(g) = 4g[K_0(2g) + K_1(2g)]e^{-2g}$ for broken time-reversal symmetry (GUE) [2,14] (for the case of multi-channel leads see Refs. [10,15]). For temperatures comparable to Δ , several resonances contribute to the same conductance peak according to (1). The

conductance peak is now affected not only by the fluctuations of the eigenfunctions but also by the statistics of the energy levels E_λ . However we can ignore the fluctuations of the energy levels to a good approximation (see below) and take a picket-fence spectrum. The conductance peak distribution can then be evaluated in closed form. Assuming the peak is positioned at $\tilde{E}_F = E_0$, the weights w_λ are fixed numbers, and only the g_λ fluctuate. Since in RMT different eigenfunctions are uncorrelated we find that the characteristic function of the conductance peak distribution $P(t) \equiv \langle e^{igt} \rangle$ is given by

$$P(t) = \begin{cases} \prod_\lambda \left(1 - \frac{itw_\lambda}{2}\right)^{-1/2} & \text{(GOE)} \\ \prod_\lambda \frac{1}{2(1 - \frac{itw_\lambda}{4})} \left[1 + \frac{\arcsin(\frac{itw_\lambda}{4})^{1/2}}{(\frac{itw_\lambda}{4})^{1/2}(1 - \frac{itw_\lambda}{4})^{1/2}}\right] & \text{(GUE)} \end{cases} \quad (6)$$

Fig. 2 shows the analytic distributions derived from (6) for both conserved (left) and broken (right) time-reversal symmetry, and for temperatures $T = 0.1\Delta$ (dotted lines), 0.5Δ and Δ (solid lines). At the lowest temperature (0.1Δ) the distributions essentially coincide with those found earlier for $T \ll \Delta$, but already at $T = 0.5\Delta$ we see a deviation. The non-interacting distributions for $T = \Delta$ are shown for comparison by the dashed lines in Fig. 2; they differ substantially from the actual $T = \Delta$ distributions. Both the mean and the variance of the conductance are suppressed at a given temperature due to the presence of the charging energy. In the inset to Fig. 2 we compare the measured distribution (solid diamonds) for non-zero magnetic field [4] with the actual distribution we calculate for $T = 0.3\Delta$ (solid line), the non-interacting distribution at $T = 0.3\Delta$ (dashed line) and the $T \ll \Delta$ distribution (dotted line). The finite temperature distribution describes correctly the dip observed in the lowest g data point. The reduced sensitivity to temperature (as compared with the non-interacting case) is already observed at this low temperature.

To test our analytic approximation (6), we have done full random matrix simulations which include the fluctuations in the single-particle energy levels as well as the possible fluctuations in the peak's position. The results are shown by the histograms in Fig. 2. The largest deviations are observed for $T = 0.5\Delta$, but even here the analytic approximation appears to work well.

Finally we calculated the peak-to-peak correlator (in a peak sequence vs. gate voltage) at finite temperature $c(n) = (\overline{G_{N_0+n}G_{N_0}} - \overline{G_{N_0}^2}) / (\overline{G_{N_0}^2} - \overline{G_{N_0}^2})$, where G_{N_0} is the conductance peak due to N_0 electrons on the dot. In the approximation that the position of each peak is fixed at $\tilde{E}_F = E_{N_0} + (N_0 - 1/2)e^2/C$ we can express $c(n)$ in terms of the weights $w_\lambda(N_0) \equiv w_\lambda(T, E_{N_0})$ given by (3) for N_0 electrons on the dot. Since in both the GOE and GUE the eigenvector distribution is independent from the eigenvalues distribution, and $\overline{g_\lambda g_\mu} = \overline{g_\lambda^2} \delta_{\lambda\mu} + \overline{g_\lambda^2} (1 - \delta_{\lambda\mu})$ where $\overline{g_\lambda}$ and $\overline{g_\lambda^2}$ are independent of λ , we find

$$c(n) \approx \frac{\overline{\sum_\lambda w_\lambda(N_0+n)w_\lambda(N_0)}}{\overline{\sum_\lambda w_\lambda(N_0)^2}}. \quad (7)$$

The remaining average in (7) is over the energy levels E_λ , although to a good approximation one can again take a picket-fence spectrum. For the latter case we can use the relation $w_\lambda(N_0+n) = w_{\lambda-n}(N_0)$ to express $c(n) \approx \sum_\lambda w_{\lambda-n}w_\lambda / \sum_\lambda w_\lambda^2$ in terms of the weights $w_\lambda \equiv w_\lambda(N_0)$ of a fixed number of electrons N_0 on the dot. The top inset of Fig. 3 shows $c(n)$ versus n for several temperatures. Fig. 3 itself shows the correlation length (defined as the full width at half maximum) as a function of temperature. The increase of the correlations between neighboring peaks with T/Δ is in qualitative agreement with the experimental results which show that the peak distributions measured at higher temperature [4] are more strongly correlated than those measured at lower temperatures [3]. The bottom inset of Fig. 3 shows a sequence of conductance peaks for a particular realization in RMT at $T \ll \Delta$ and $T = 0.5\Delta$. Nonetheless, the peak series in Ref. [4] exhibits even stronger peak correlations than we would expect for the estimated temperature of $T \approx 0.3 - 0.5\Delta$. The origin of this enhancement of the correlations at low temperatures is not fully understood [16].

In conclusion, using RMT we have derived the finite temperature conductance peak height distributions and peak-to-peak correlations in Coulomb blockade quantum dots. The charging energy was shown to affect the distribution of the conductance peaks at finite temperature when compared with the results of a non-interacting theory. Further measurements of the mesoscopic fluctuations of the conductance at temperatures comparable to the mean

level spacing are necessary for a detailed comparison with our theoretical results.

This work was supported in part by the Department of Energy grant No. DE-FG-0291-ER-40608 and by NSF grant DMR-9215065. We thank A. Chang and C.M. Marcus for helpful conversations.

REFERENCES

- [1] For a review see for example, M.A. Kastner, Rev. Mod. Phys. **64**, 849 (1992); W.P. Kirk and M.A. Reed (Ed.), *Nanostructures and Mesoscopic Systems* (Academic Press, San Diego, 1992).
- [2] R.A. Jalabert, A.D. Stone, and Y. Alhassid, Phys. Rev. Lett. **68**, 3468 (1992).
- [3] A.M. Chang, H.U. Baranger, L.N. Pfeiffer, K.W. West and T.Y. Chang, Phys. Rev. Lett. **76**, 1695 (1996).
- [4] J.A. Folk, S.R. Patel, S.F. Godijn, A.G. Huibers, S.M. Cronenwett, C.M. Marcus, K. Campman and A.C. Gossard, Phys. Rev. Lett. **76**, 1699 (1996).
- [5] Y. Alhassid and H. Attias, Phys. Rev. Lett. **76**, 1711 (1996).
- [6] R. Landauer, IBM J. Res. Dev. **1**, 223 (1957); Philos. Mag. **21**, 863 (1970); M. Büttiker, Phys. Rev. Lett. **57**, 1761 (1986); IBM J. Res. Dev. **32**, 317 (1988).
- [7] C.W.J. Beenakker, Phys. Rev. B **44**, 1646 (1991).
- [8] D.V. Averin, A.N. Korotkov and K.K. Likharev, Phys. Rev. B **44**, 6199 (1991).
- [9] H. Bruus and A. D. Stone, Phys. Rev. B **50**, 18275 (1994).
- [10] Y. Alhassid and C.H. Lewenkopf, Phys. Rev. Lett. **75**, 3922 (1995).
- [11] W. E. Ormand, D. J. Dean, C. W. Johnson, G. H. Lang and S. E. Koonin, Phys. Rev. C **49**, 1422 (1994).
- [12] A. Kamenev and Y. Gefen, Chaos, Solitons and Fractals **8**, 1229 (1997).
- [13] Note that w_λ are symmetric around $\lambda = 0$, which is a result of the interesting relation $\langle n_{-m} \rangle (1 - f(E_{-m} - E_0)) = \langle n_m \rangle (1 - f(E_m - E_0))$, valid for any spectrum which is symmetric around the central level.
- [14] V. N. Prigodin, K. B. Efetov, and S. Iida, Phys. Rev. Lett. **71**, 1230 (1993).

- [15] E.R. Mucciolo, V.N. Prigodin, and B.L. Altshuler, Phys. Rev. B **51**, 1714(1995).
- [16] There are two possible explanations that require further studies to be substantiated: (i) Self-consistent density functional calculations (M. Stopa, Phys. Rev. B **54**, 13767 (1996); and private communication) of the single-particle spectrum of dots find approximately periodic oscillations of the level density near E_F as N increases. Therefore in certain regions of gate voltage the effective value Δ would be smaller than the average value, leading to anomalously large correlations (due to an effectively larger value of T/Δ). (ii) The enhancement is due to spin-paired levels. Such levels are inferred to exist from the presence of nearby levels with very similar magnetoconductance traces (S. Patel et al, to be published).

FIGURES

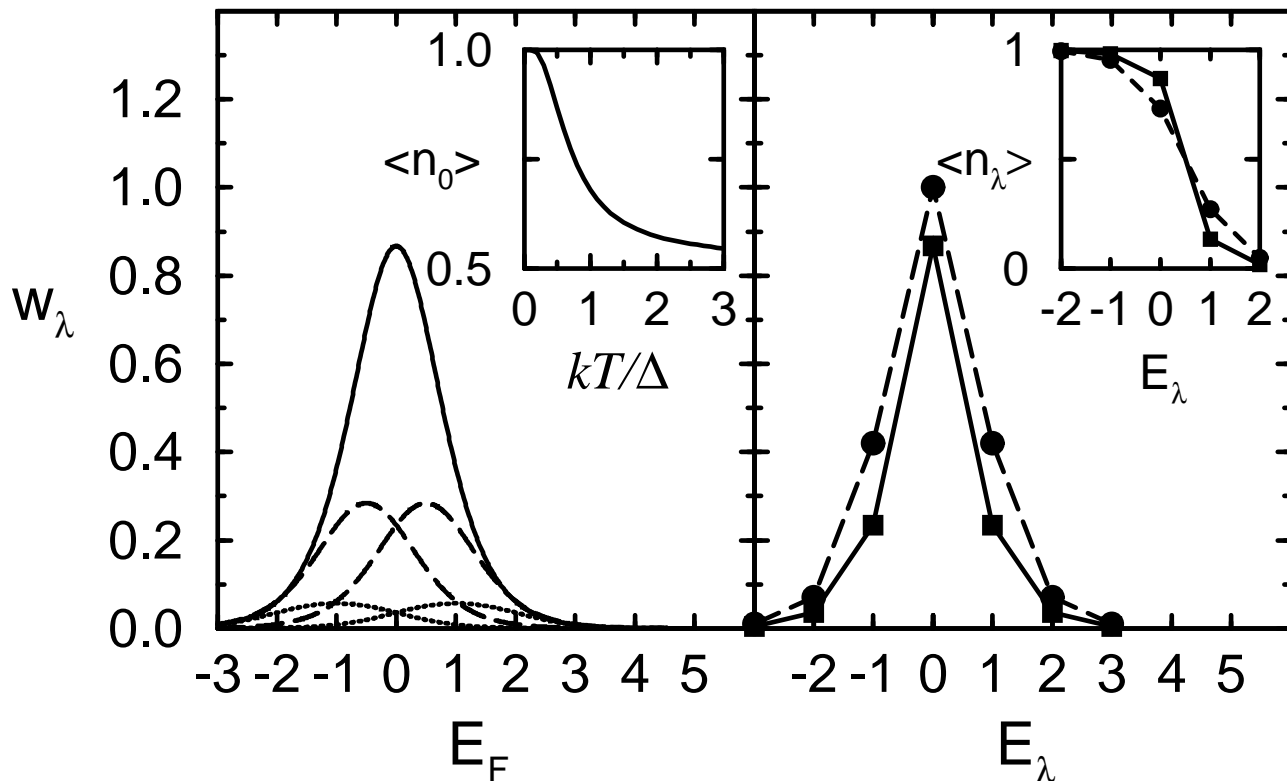


FIG. 1. Left: The weights $w_\lambda(T, \tilde{E}_F)$ versus \tilde{E}_F at $T = 0.5\Delta$ and for resonance levels $\lambda = 0$ (solid line), ± 1 (dashed lines), ± 2 (dotted lines) assuming a picket-fence spectrum. Right: The weights w_λ (Eq. (3), solid squares) at $\tilde{E}_F = E_0$ versus E_λ in comparison with the non-interacting weights w_λ^{LB} (solid circles). The right inset shows the canonical occupations $\langle n_\lambda \rangle$ (solid squares) versus E_λ in comparison with a Fermi-Dirac distribution (dashed line). The left inset shows $w_0 = \langle n_0 \rangle$ as a function of temperature.

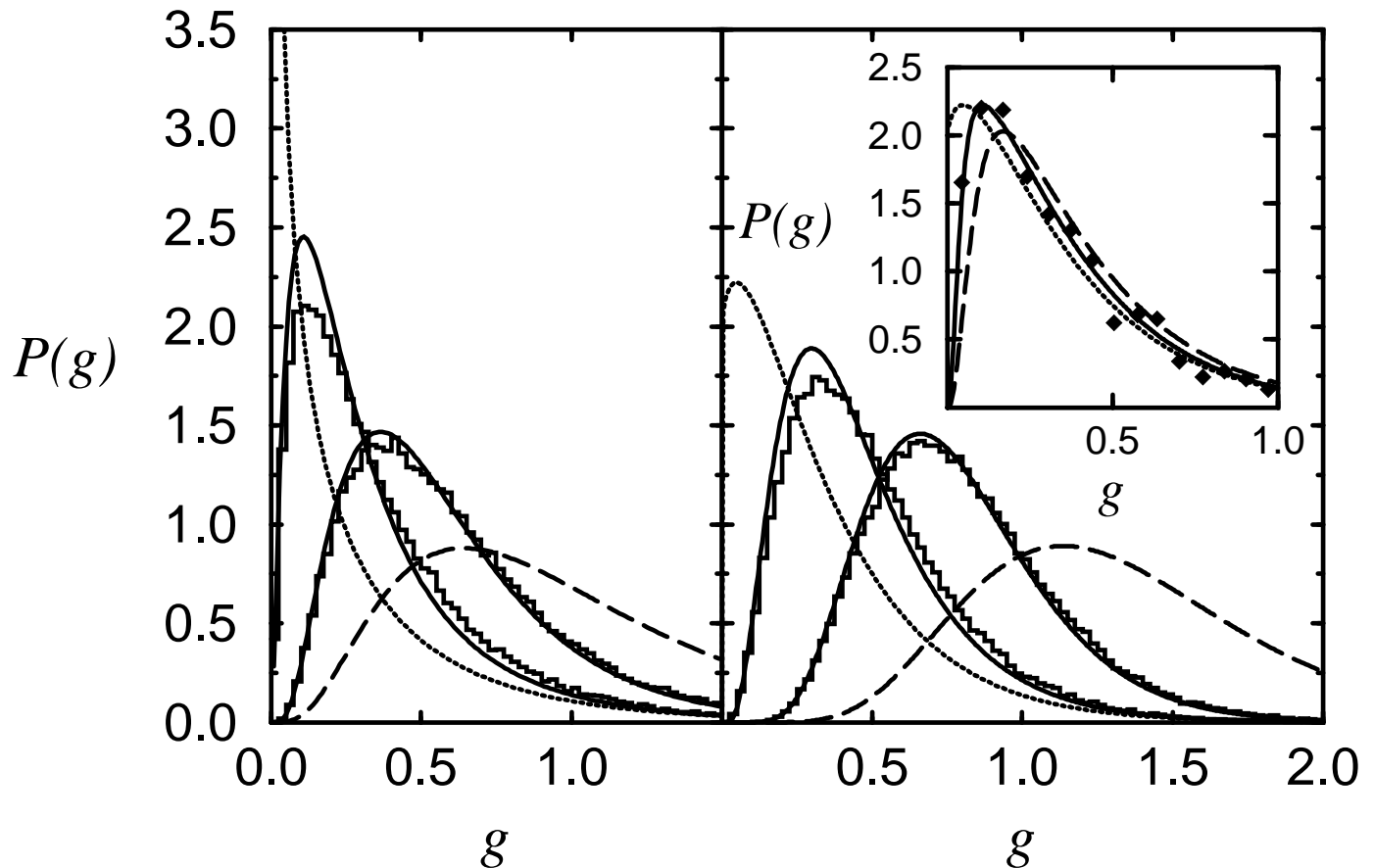


FIG. 2. The conductance peak height distributions $P(g)$ for the GOE (left) and GUE statistics (right). The solid lines are the analytic distributions (see (6)) at $T/\Delta = 0.5, 1$ for a picket-fence spectrum using the weights (3), while the histograms describe the respective distributions obtained from full RMT simulations (see text). For comparison we also show the $T \ll \Delta$ distributions (dotted lines) and the non-interacting distributions for $T = \Delta$ (dashed lines). The inset compares the experimental distribution in the presence of magnetic field [4] (diamonds) with the $T = 0.3\Delta$ GUE distribution (solid line), the $T = 0.3\Delta$ non-interacting distribution (dashed) and the $T \ll \Delta$ distribution (dotted).

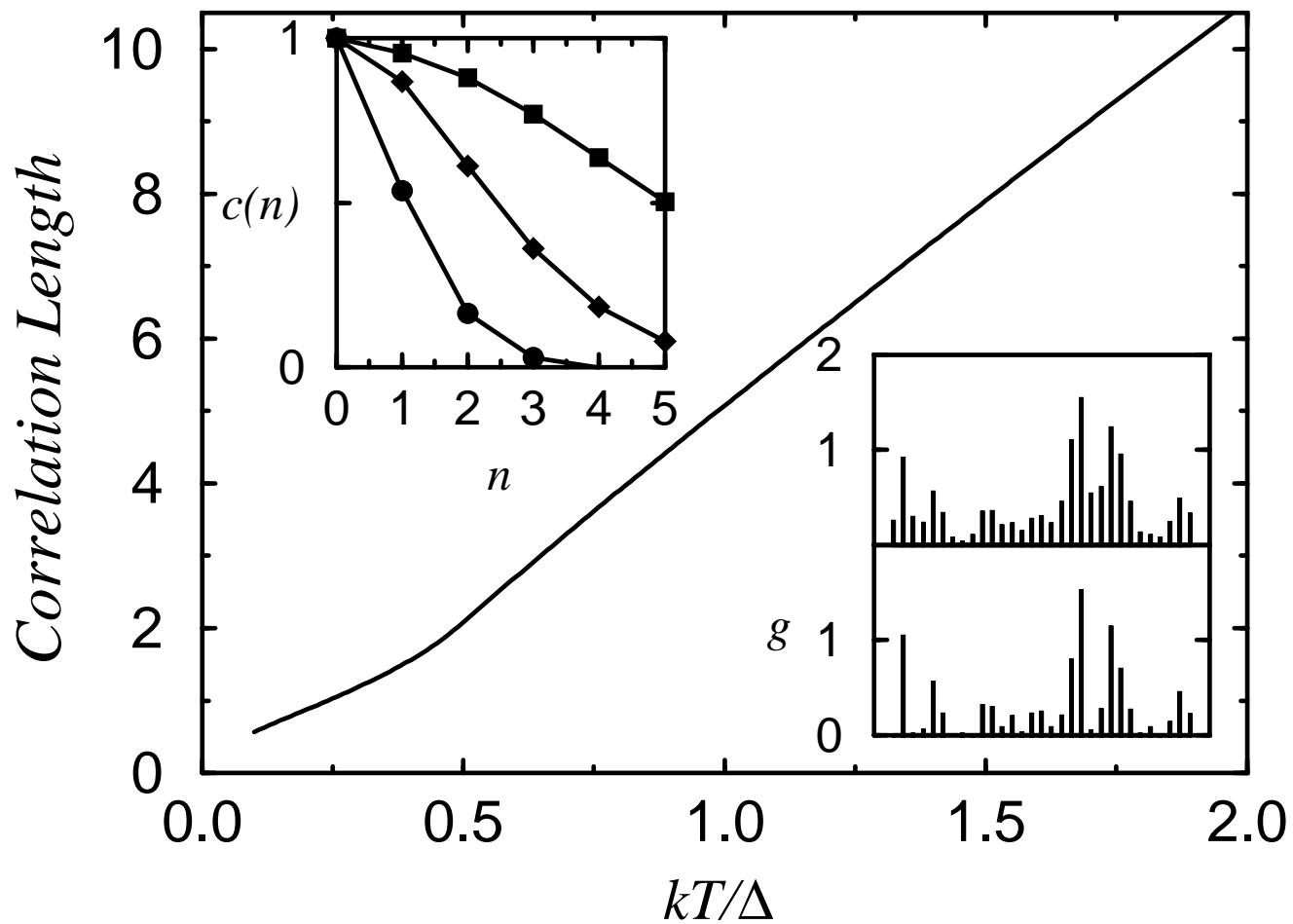


FIG. 3. The correlation length (full width at half maximum) of the peak-to-peak correlator $c(n)$ as a function of temperature. Left inset: $c(n)$ versus peak separation n at several temperatures $T/\Delta = 0.5, 1, 2$. Right inset: a realization of an RMT peak sequence at $T \ll \Delta$ (bottom part) and $T = 0.5\Delta$ (top part).